ACS central science

Research Article

Cite This: ACS Cent. Sci. 2019, 5, 357−364

http://pubs.acs.org/journal/acscii

On Biomineralization: Enzymes Switch on Mesocrystal Assembly

Ashit Rao,[†,‡] Teresa Roncal-Herrero,[§,∥] Elina Schmid,[†] Markus Drechsler,[⊥] Martin Scheffner,[#] Denis Gebauer,[†] Roland Kröger,[§] and Helmut Cölfen*[,†]

[†]Physical Chemistry, Department of Chemistry, University of Konstanz, Universitätsstr. 10, Konstanz 78464, Germany

[‡]Faculty of Science and Technology, Physics of Complex Fluids, University of Twente, PO Box 217, Enschede 7500 AE, The Netherlands

[§]Department of Physics, University of York, Heslington YO10 5DD, United Kingdom

[∥]School of Chemical and Process Engineering, University of Leeds, 211 Clarendon Road, Leeds LS2 9JT, United Kingdom

[⊥]Bavarian Polymer Institute, Keylab Electron and Optical Microscopy, University of Bayreuth, Universitätsstr. 30, Bayreuth 95440, Germany

[#]Cellular Biochemistry, Department of Biology, University of Konstanz, Universitätsstr. 10, Konstanz 78464, Germany

Supporting Information

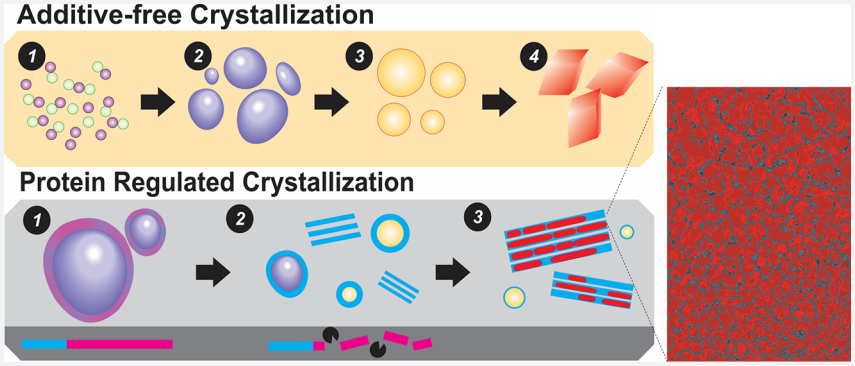

ABSTRACT: Cellular machineries guide the bottom-up pathways toward crystal superstructures based on the transport of inorganic precursors and their precise integration with organic frameworks. The biosynthesis of mesocrystalline spines entails concerted interactions between biomolecules and inorganic precursors; however, the bioinorganic interactions and interfaces that regulate material form and growth as well as the selective emergence of structural complexity in the form of nanostructured crystals are not clear. By investigating mineral nucleation under the regulation of recombinant proteins, we show that SpSM50, a matrix protein of the sea urchin spine, stabilizes mineral precursors via vesicle-confinement, a function conferred by a low-complexity, disordered region. Site-specific proteolysis of this domain by a collagenase initiates phase transformation of the confined mineral phase. The residual C-type lectin domain molds the fluidic mineral precursor into hierarchical mesocrystals identical to structural crystal modules constituting the biogenic mineral. Thus, the regulatory functions of proteolytic enzymes can guide biomacromolecular domain constitutions and interfaces, in turn determining inorganic phase transformations toward hybrid materials as well as integrating organic and inorganic components across hierarchical length scales. Bearing striking resemblance to biogenic mineralization, these hybrid materials recruit bioinorganic interactions which elegantly intertwine nucleation and crystallization phenomena with biomolecular structural dynamics, hence elucidating a long-sought key of how nature can orchestrate complex biomineralization processes.

INTRODUCTION

Nature's toolbox for material genesis inspires synthetic routes toward functional materials with intricate morphologies, patterns, and organizations.[1−6] Biogenic pathways exhibit exquisite control over the size and structure of hybrid materials across several length scales. However, a lacuna of understanding persists for bioinorganic interactions of functional and regulatory significance that underlay the development and organization of biomaterials. In consideration of biologically controlled nucleation and crystallization, the formation and (de)stabilization of metastable amorphous mineral precursors, mechanisms of phase transformation as well as the sophisticated unification of organic and inorganic building units into functional mesostructured materials represent fascinating, however less understood, fundamental aspects of biomineralization.

Received: November 19, 2018
Published: February 1, 2019

DOI: 10.1021/acscentsci.8b00853
ACS Cent. Sci. 2019, 5, 357−364

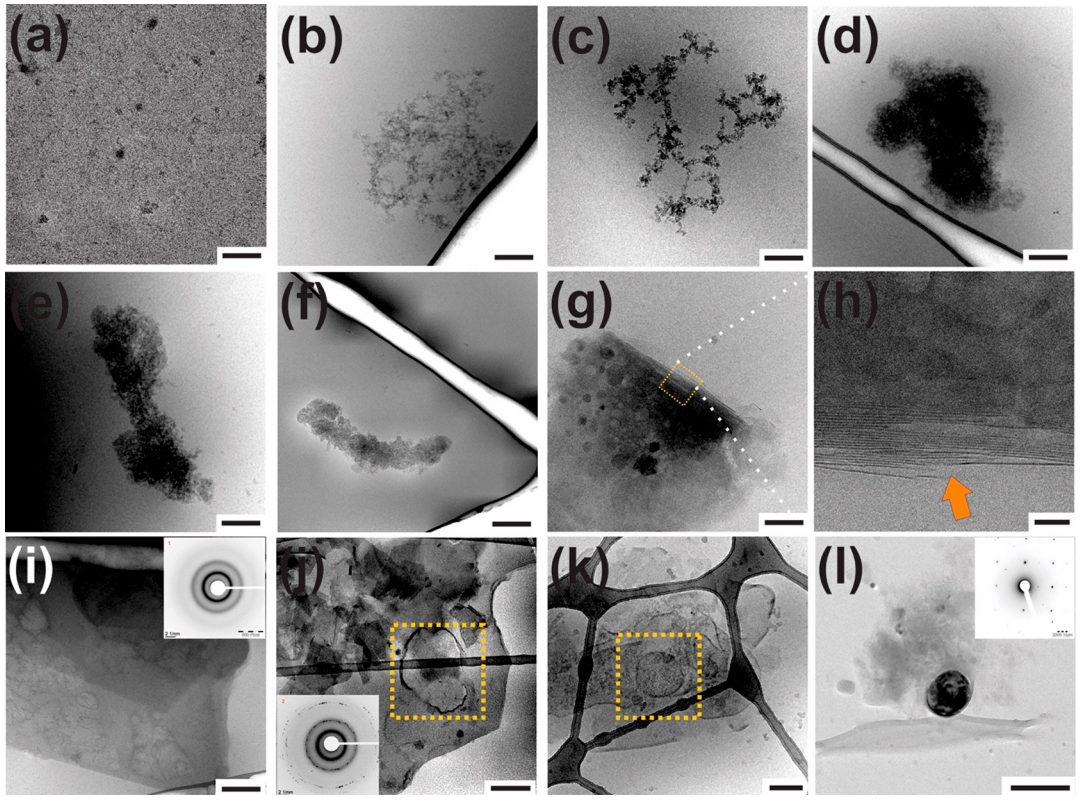

Figure 1. Representative cryo-TEM micrographs corresponding to the (a–f) prenucleation stages and (g–k) postnucleation stages for mineral nucleation during CTLD-controlled nucleation at pH 9.0 with protein contents of 0.1 mg/mL. Presence of organic laminae (g and h) and vesicular structures (j and k) are indicated. (l) Representative TEM image and corresponding ED pattern of a nucleated particle. Scale bars represent (a and i) 100 nm, (b–e, k, and l) 200 nm, (f and j) 0.5 μm, and (h) 10 nm.

Structural studies on calcareous elements from echinoderms have shed some light on biomineralization pathways. Constructed by the transport and transformation of amorphous precursors, the sea urchin spine emerges as a biogenic mesocrystal composed of co-oriented calcite particles organized in a space-filling manner within a cement of amorphous mineral and biomolecules.[5,7−9] This superstructure reconciles seemingly inconsistent material properties that enable a single crystal-like diffraction behavior and concomitantly a conchoidal fracture behavior typical of amorphous materials.[7] Having explored structure−property relations of these biominerals, the extent of biochemical and biophysical regulation imposed upon nucleation and crystallization reactions toward achieving hybrid crystalline superstructures requires attention.

The intricate organic−inorganic interactions involved in sea urchin skeletogenesis is reflected by the diversity of biomineral-associated macromolecules.[10,11] Of these, SpSM50 is an abundant nonglycosylated matrix protein in the organic matrix of the sea urchin spine.[10] Localized in Golgi membranes and extracellular mineralization compartment as well as occluded within the biomineral, SpSM50 is potentially multifunctional, regulating early nucleation stages and subsequent phase transitions of the mineral phase. Recent investigations also indicate that spine-associated proteins modulate the early regime of mineral nucleation, inhibiting nucleation and transiently stabilizing amorphous minerals and also forming assemblies and hydrogels, which can control the texture and internal structures of emergent mineral crystals.[12−15] Exemplified by proteins such as SpSM50, PM27, SM29, and the SM30 family, the prevalence of C-type lectin-like domains (CTLDs) in the biomineral proteome suggest distinct contributions toward mineralization.[10,11,16] In this manner, the functional aspects of specific nanoscopic bioinorganic interactions and interfaces as well as the relative positions of biomolecular players in the regulatory cascade of mineral nucleation and crystallization require further elucidation.

Recent developments in the field of nucleation and crystallization suggest that early mineralization events involving ion clusters, liquid condensed phases, and amorphous particles significantly contribute to the selective emergence of crystal form, structure, and organization.[17−20] It is important to address the structural dynamics and post-translational modifications of the biomacromolecules in relation to these distinct crystal precursors and their microenvironments under well-defined experimental conditions. Our interdisciplinary approach involves the application of recombinant biomineral-associated proteins in a mineralization protocol that enables precise control over solution parameters, in situ quantitative insights into the nucleation process, and time-dependent reaction sampling. The structural evolution of organic−inorganic complexes is accessed by using analytical ultracentrifugation (AUC) and liquid cell (LC−)/cryogenic transmission electron microscopy (cryo-TEM). Collectively, these techniques construct a holistic overview of bioinorganic interactions involving distinct mineral precursors of solute, fluidic, and particulate compositions.[18,21,22] Given the indispensable role of the spicule matrix protein, SpSM50, in spine development,[23] recombinant forms of the full-length protein and its constitutive domains (Figure S1) are purified as fusion products[14] and applied as mineralization additives. An N-terminal small ubiquitin-like modifier (SUMO)

DOI: 10.1021/acscentsci.8b00853
ACS Cent. Sci. 2019, 5, 357−364

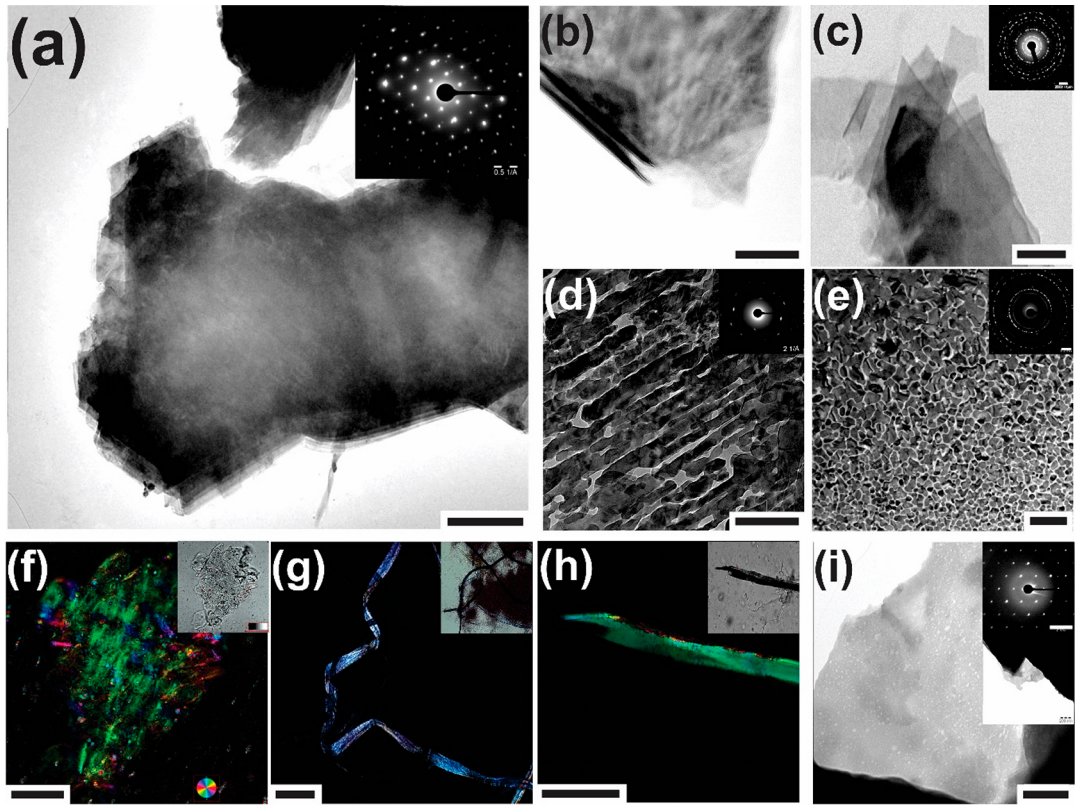

Figure 2. Representative TEM micrographs of (a and b) CTLD-mediated multilaminar mesocrystals formed during mineral nucleation at pH 9. Mesocrystal deconstruction by (c) sonication, (d) ultramicrotomy, or (e) proteinase K treatment reveals crystallographic co-orientation between particles of adjacent laminae and a space-filling nanoparticle arrangement. (f) Color-mapped crystallographic spread of a wet mount mesocrystal by quantitative polarization microscopy. Structural analyses of the constituents from the adult spine of *Strongylocentrotus purpuratus* by means of (g) dark field polarization light microscopy, (h) quantitative polarization microscopy, and (i) TEM. Insets represent (a, c–e, and i) ED patterns, (f–h) bright-field images, and (i) TEM image at lower magnification. Scale bars represent (a) 1 μm, (b–e and i) 200 nm, (f) 50 μm, (g) 100 μm, and (h) 20 μm.

tag is utilized because of the high aggregation propensity and toxicity of untagged biomineral-associated proteins. Note the unique domain architecture of SpSM50 (Figure S1), with a folded N-terminal CTLD and a highly basic disordered glycine and proline rich domain (GRR).

RESULTS AND DISCUSSION

Under nonreducing conditions, the recombinant C-type lectin-like domain is ascertained as well-folded, with conformational responses to Ca^{2+} ions and functionality toward sugar binding (Figure S2). The affinity of the CTLD with specific sugar residues has mechanistic implications toward heterointeractions guiding the construction of organic scaffolds during biomineralization.[13,24,25] The protein is applied during calcium carbonate ($CaCO_3$) nucleation in a potentiometric titration setup.[21] Distinct nucleation profiles are elicited by the CTLD, determined by the conditions of solution pH as well as protein concentration, conformation, and redox states (Supporting Information, section 3). Considering the four cysteine residues in the CTLD sequence, the dependence of mineral nucleation profiles on redox environments reflect the complementarity and specificity of bioinorganic interactions between the solvent exposed amino acid residues of the CTLD and inorganic species such as ions, ion-clusters, and liquid-like and particulate precursors.[18,20] During the progression of mineralization, the protein molecules cluster and mature in terms of size and density, as observed by cryo-TEM of samples collected at different nucleation stages (Figure 1). In the prenucleation regime (i.e., before the formation of solid mineral particles), protein-ion complexes become denser and self-associate, presenting size developments from about 10 nm to 5 μm. From ion complexation studies as well as dynamic light scattering and analytical ultracentrifugation, the observed structural transitions of the CTLD appear to be collectively driven by single ions, ion-clusters, and emergent mineral precursors, forming larger, asymmetric biomolecular self-associates for the latter (Supporting Information section S4). Following mineral nucleation, the CTLD protein forms sheet-like structures, which stack and form organic laminae (Figure 1h, arrow). Free Ca^{2+} ions also induce CTLD self-association toward sheet-like microstructures, although over longer time periods, indicating that the dynamics of ionic and pH conditions during mineral nucleation can enhance the kinetics of macromolecular self-association and supramolecular assembly (Figure S4C). Interestingly, certain lectins produce similar sheet-like nanostructures induced by divalent cations, wherein multiple factors such as sequence composition and structural dynamics contribute to the emergence of supramolecular organizations.[26] As shown in Figure 1, the contributions of vesicular structures in the mineralization of the laminae assemblies are supported by spatial proximity to mineralized bodies and the drying-induced crystallization of vesicles toward calcite.[19] Considering that scaffold self-assembly precedes crystallization of the inorganic phase and also the high solubility of the initially nucleated mineral phase deduced from titration experiments (Figure S3B), the mechanistic roles of the

DOI: 10.1021/acscentsci.8b00853
ACS Cent. Sci. 2019, 5, 357–364

capillarity associated with liquid-like mineral precursors can contribute to mineralization of the laminar scaffold.[18,27] In view of the conformational stability of the CTLD toward Ca^{2+} ions as well as the distinct ion-association behavior (Figures S2 and S4A), factors such as ion bridging and hydrophobic interactions appear to induce macromolecular self-assembly and the subsequent emergence of functional bioinorganic interfaces.

Subsequent to mineral nucleation, a structural transition occurs from proteinaceous sheets to multilamellar composites, which exhibit ED patterns typical of monocrystalline calcite (Figures 2a and S5). The CTLD stabilizes the high-energy (001) calcite face, indicating that the protein actively interfaces with the crystalline phase, intrinsically reinforcing a mesocrystalline architecture (Figure S5). Detailed structural evaluation of titration-derived composites reveals a unique multilamellar mesocrystal exhibiting two distinct levels of hierarchy (Figure 2). First, mechanical disruption of the laminar organization produces crystallographic misaligned composite structures (Figure 2c,d). This reflects the co-orientation of crystalline domains constituting adjacent laminae. Second, the protease-mediated elimination of CTLD from single lamina produces a space-filling arrangement of irregular, calcite particles (Figures 2e and S5B), consistent with structural accounts of the biogenic mineral.[7,28] AFM characterization of the demineralized organic template presents porous topographies, which structurally complements the dimensions of the mineral nanoparticles (Figure S5B). Thus, the mineralization-induced self-association of CTLD provides an organic framework conducive for the integration of inorganic constituents and organic assemblies toward crystalline, laminar composites.

Sedimentation velocity experiments provide solution-state insights into the bioinorganic interactions that underlay mesocrystal formation, wherein global pH and ionic conditions related to mineral nucleation augment CTLD self-assembly toward asymmetric shapes with high frictional ratios (Figure S4B). Under the applied chemical environments, the optimal stoichiometry for Ca^{2+} ion binding corresponds to less than one divalent ion for each carboxylate group within a protein monomer (about 0.1 Ca^{2+} ion for each aspartate/glutamate residue at pH 9.0). This suggests that non-Coulomb interactions such as hydrophobic forces also contribute to nanoscale interactions that underlay supramolecular architectures.[29] In view of the mineralization process, the titration estimated solubility products of the nucleated mineral phases (Figure S3B), time-dependent polarization microscopy imaging (Figure S5C), and the analogous mosaic patterns with materials derived from liquid-phase sintering (Figure 2e) collectively indicate the recruitment of biochemically stabilized hydrated, transient mineral precursors. In agreement, the presence of vesicular structures encompassing mineral precursors suggests the contributions of protein-stabilized liquid condensed phases in the crystallization reaction.[19,22] Associated organic−inorganic phases can provide a viscous environment for grain coarsening, densification, and oriented attachment processes.[5,6,18] We also reveal the transient stability of the mesocrystals using X-ray scattering, wherein the average thickness of mineralized laminae grows from 1.6 to 8.3 nm to above 100 nm with increasing time (Figure S5B). This structural evolution is attributed to the coalescence of mesocrystal building units to form larger crystalline domains, hence reflecting the kinetic stability of calcareous mesostructured architectures. Exploring similarities to the biological counterpart, the controlled deconstruction of the biogenic spine material reveals multilamellar, ribbon-like components with ED patterns suggestive of the [001] zone axis orientation of calcite (Figure 2). The nanoporosities decorating the ribbon surfaces also reflect a space-filling arrangement of constitutive nanoparticles. Overall, analogous structural and crystallographic features exhibited by the biomimetic and biogenic mesocrystals reveal the participation of the CTLD in bridging mineral nanocrystals within architectures exhibiting multiple levels of structural hierarchy. In this light, the remarkable superstructure of this biomimetic mineral might elucidate the prevalence of CTLDs among the members of the spicule proteome.[16]

Abundant within hierarchical biominerals, the mechanistic contributions of low-complexity, disordered (LCD) domains are implied in regulating biomineralization, exhibiting distinct phase behavior as fluidic or hydrogel materials[12,30] and disorder-to-order transitions toward functional nanostructures.[13,19,30,31] Recently, the LCD module of SpSM50 is shown to transiently stabilize an amorphous mineral precursor via vesicular confinement in analogy to the CTLD-mediated structures, however presenting better transient stabilities.[19] Interestingly, vesicular structures confining mineral precursors also contribute to the development of the sea urchin spine.[8,32] By applying density gradients during analytical ultracentrifugation, we derive the core−shell parameters of the LCD domain-stabilized vesicles, yielding values of 6.4 ± 2.5 nm and 1.399 ± 0.001 g/cm^3 corresponding to the shell thickness and core density, respectively (Supporting Information section 6). The shell thickness suggests transitions from bilayer to multilayer protein shell architectures, induced by protein self-association and distinct interactions directed toward inorganic interfaces in the course of mineral nucleation. A bilayered shell also indicates the amphiphilic structure of the recombinant protein, originating from the globular N-terminal domain and the extended, more hydrophobic disordered region.[12,14] On the other hand, the core is constituted by a highly hydrated amorphous mineral phase, with a 20−50% higher hydration content and a density considerably lower than that of hydrated amorphous $CaCO_3$ (ACC; 1.49−1.62 g/cm^3).[33,34] Given the possibility of protein molecules incorporated in the confined phase, the actual enhancement in mineral hydration contents relative to ACC is possibly greater. The estimated density of gel-like mineral precursors stabilized by small charged molecules is lower, about 1.2 g/cm^3;[35] hence, in the present study, the incorporation of protein species within the stabilized mineral core is plausible. In this regard, the confinement of highly hydrated mineral precursors appears to emerge from the localized self-assembly of biomolecules at the interfaces of kinetically stabilized nascent mineral nanodroplets, also reflecting fundamental contributions of confinement-mediated phase stabilization with morphological similarities to vesicles observed in vivo.[19,22,32,36,37] In verification of the proposed mechanism, the simulation of mineralization-induced vesicles is performed by exposing rhodoamine-labeled SpSM50 to water:THF mixtures.[19] Line plots of the fluorescence signal show the exclusion of proteins from the vesicle core, hence revealing the contributions of transient liquid−liquid interfaces as well as an antisolvent component in establishing vesicle shells (Figure S6C). Such conditions can be translated to mineralization scenarios, wherein divalent ions and their solute clusters aggravate protein solubility. Subsequently, the interfaces of nascent mineral droplets and particles provide adsorption sites for these preconditioned macromolecules, in the present study producing hybrid vesicular structures. Comparison of the CTLD- and

DOI: 10.1021/acscentsci.8b00853
ACS Cent. Sci. 2019, 5, 357−364

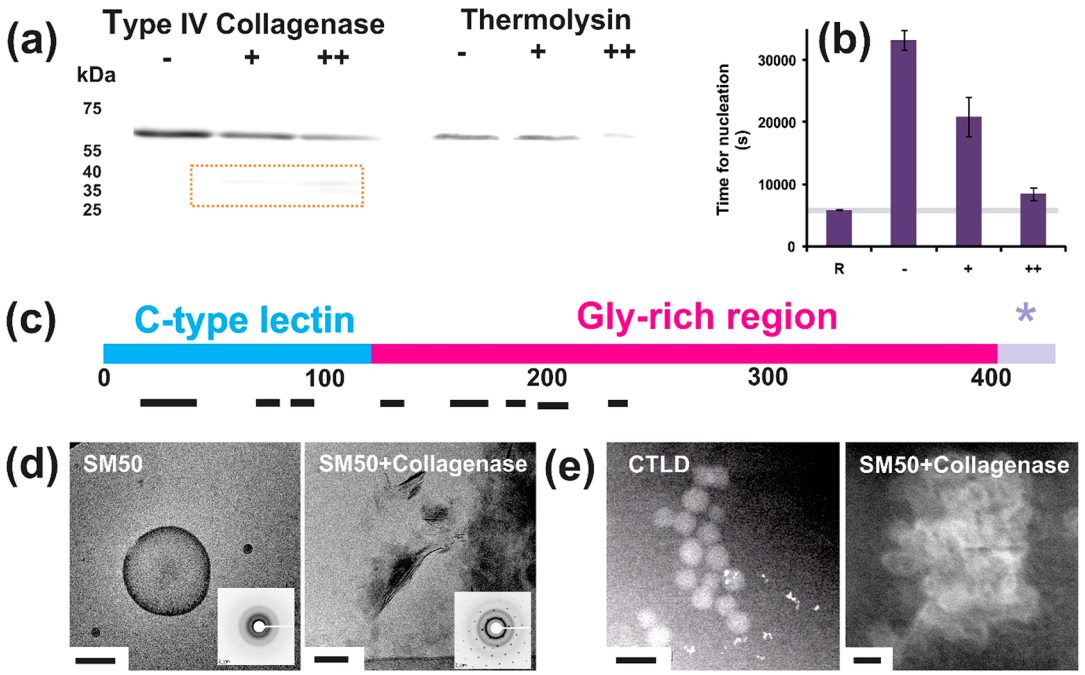

Figure 3. (a) Western blots representing the proteolytic susceptibility of SM50 toward type VI collagenase and thermolysin developed using anti-SM50 polyclonal antibodies and protease contents of 10 (+) or 100 (++) μg/mL. (b) Time required for mineral nucleation in reference experiments (R) and in mineralization solutions containing only 1 mg/mL SM50 (−) and also supplemented with type VI collagenase. (c) Black bars represent the sequence coverage of SM50 proteolytic products produced by collagenase activity (box a). (d) Representative cryo-TEM images of mineral products formed in the presence of SM50 alone and in combination with a type VI collagenase. (e) Snapshots of mineralization reactions in the presence of the CTLD (Supplementary Video 1) or a SM50/type VI collagenase mixture acquired by using LC-STEM. Note the high aggregation propensity of vesicles and their hollow cores in the presence of collagenase. Scale bars represent (d) 500 (left) and 200 (right) nm and (e) 100 nm.

SpSM50- or GRR-controlled mineral nucleation phenomena shows that the hybrid supramolecular architectures are markedly distinct in form, structure, and crystallinity, with the inorganic phase inducing unique variations in the conformational and self-association states of the organic precursors. Therefore, during biomineralization, the organic−inorganic interactions encompassing biomolecular conformation and self-organization appear chemically programmed and elicit distinct nucleation and crystallization responses in relation to the physical states, interfaces, and structures of the maturing mineral phase viz. ions, ion-clusters, liquid condensed phases, and amorphous and crystalline particles. Following an analogous pathway, the structural transitions for the investigated proteins proceed from soluble species to discrete self-associates of higher order such as rods, sheets, and laminae (Figures 1 and S6A). In this sense, biomineralization phenomena appear to encompass "nonclassical pathways" for both the inorganic and organic phases, wherein the bioinorganic interface is highly dynamic, constituted with hybrid precursors with transient degrees of self-association, solvation, and structural dynamics that navigate across a highly complex energetic landscape to the final composite phase and organization.

To address the incongruous effects of the constitutive domains of SpSM50, i.e., the CTLD mediating mesocrystal formation and the LCD region effectively stabilizing mineral precursors within vesicles, we further characterize the mineralization behavior of the full-length protein. Previous studies show that sea urchin embryos exposed to inhibitors of matrix metalloproteases (MMPs) exhibit vesicle accumulation in the cytoplasm of mesenchymal cells and arrested biomineral development.[38] Biochemical analyses of proteins from sea urchin skeletal elements also identify SpSM50 fragments at low molar masses relative to the full length version.[16,39] These studies suggest that matrix metalloproteases participate in the maturation of biomineralization proteins, for instance enhancing the integration of partially proteolyzed macromolecules into growing crystals.[16] This hints that extracellular matrix modeling in the context of homeostatic biomineralization necessitates selective proteolytic processing. Along this line, we examine the in vitro susceptibility of the recombinant SpSM50 toward proteolysis by a type IV collagenase (Figure 3a,c) and the sequence coverage of residual fragments (Supporting Information section 7), thus revealing a selective degradation of the LCD and a relative conservation of the CTLD. Western blots of spine extracts developed using CTLD-specific primary antibodies also produce a 15 kDa fragment corresponding to the lectin domain, in addition to the full-length protein (Figure S8B).

With the disordered domain of SpSM50 identified as a putative target of proteolysis, the consequences of this post-translational processing on mineral formation are addressed. In reference experiments, the full-length SpSM50 significantly inhibits mineral nucleation and transiently stabilizes a highly soluble mineral phase (Figures 3 and S8A). Consistent with the reported stabilization of a hydrated amorphous mineral precursor,[12,40] here we identify the functional contributions of vesicular confinement in stabilizing the mineral precursor against crystallization (Figure 3). Similar nucleation profiles elicited by the full-length SpSM50 and its constitutive LCD domain and a likewise vesicular entrapment of amorphous mineral precursor within proteinaceous bodies[19] indicate that the independent effects of the disordered region on mineral nucleation supersede those of CTLD. However, combined applications of the matrix protein and collagenase in mineralization experiments diminish the time periods (i.e.,

DOI: 10.1021/acscentsci.8b00853
ACS Cent. Sci. 2019, 5, 357−364

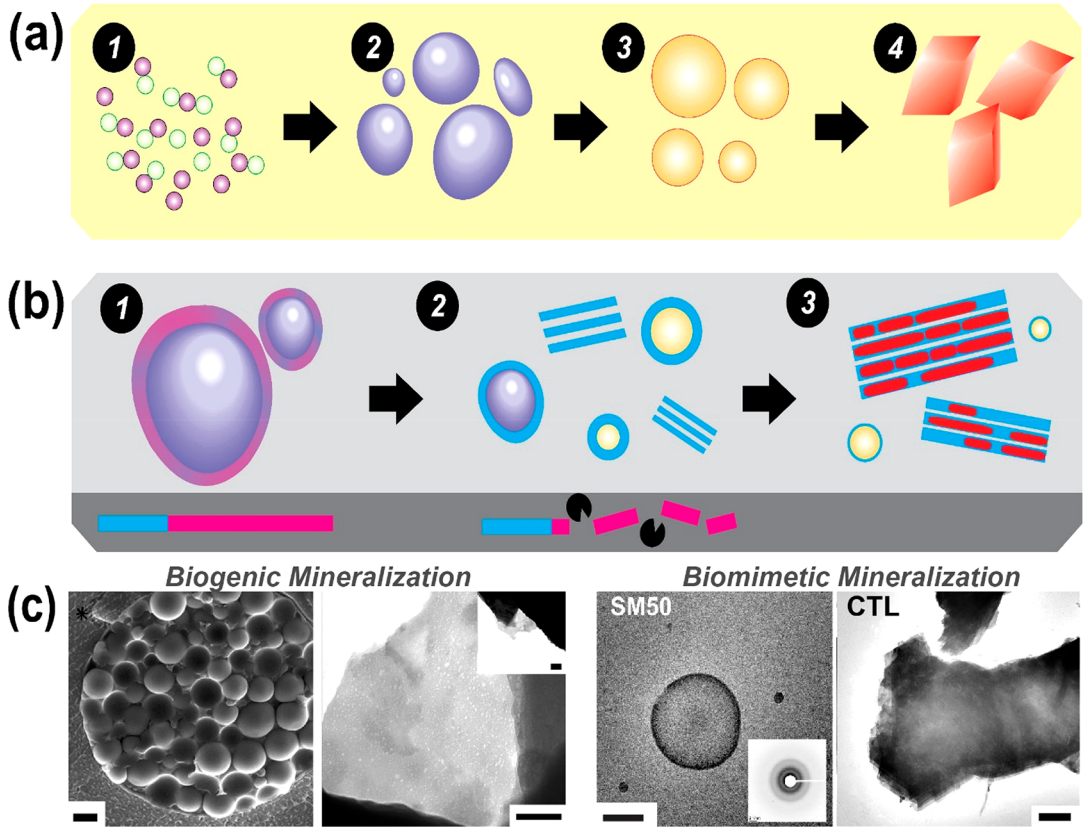

Figure 4. (a) Scheme illustrating different stages of the formative process of crystalline minerals involving (1) a population of stable, structurally dynamic ion-clusters, (2) at a critical ion activity, the liquid−liquid demixing of mineral nanodroplets and the subsequent nucleation of (3) amorphous calcium carbonate and (4) crystalline polymorphs. (b) Schematic representation of the multifunctionality of SM50 (1) initially forming vesicles that confine and stabilize a liquid-like amorphous mineral form. (2) At the site for mineral growth, MMP activity specifically cleaves the disordered domain of SM50 (pink), which is crucial for vesicle stability. This initiates the phase transformation of the amorphous phase to calcite under regulation of the residual CTLD (blue). Conditions of pH and supersaturation drive the assembly of CTLD to scaffolding structures. (3) The destabilized fluidic (and possibly transient particulate[45,46]) precursors infiltrate and mineralize the organic laminae, generating calcite mesocrystals. (c) Structural similarities between vesicles trafficking mineral precursors and laminar modules from the sea urchin spine (left) to SM50-based vesicular structures and CTL-mediated calcite mesocrystals (right). Scale bars represent 1 μm, 200 nm, 500 nm, and 1 μm, left to right. (*The left-hand image in panel c is reproduced with permission from ref 32. Copyright 2014 National Academy of Sciences.)

supersaturation conditions) required for the nucleation of mineral particles in comparison to SpSM50 alone, an effect accentuated by increasing protease contents (Figures 3 and S8). Similar structural transitions from vesicles to mesocrystalline laminae are also identified in the presence of either the CTLD alone or SpSM50-collagenase mixtures (Figures 3 and S8B). The coapplication of SpSM50 and the protease leads to the formation of laminar mesocrystals that present single crystal-like diffraction and polarization patterns. Last, LC-STEM experiments demonstrate the existence of transient vesicles during mineralization performed in the presence of SpSM50 and type VI collagenase mixtures as well as for CTLD alone (Figure 3). In this manner, the crystalline products of the protease-guided mineralization pathway are structurally similar to the CTLD-mediated mesocrystals. Hence, the quantitative mineralization experiments as well as the morphological and structural evaluation of the resultant mineral structures reveal that a "switching-on" of CTLD-controlled mesocrystal formation occurs in the presence of a MMP (Figure 4).

For biochemically guided mineralization pathways, proteolysis emerges as an important post-translational checkpoint guiding the nucleation and crystallization of inorganic phases. This mode of regulation involves distinct consequences for bioinorganic entities recruiting ion, ion-clusters, fluidic mineral phases, as well as amorphous and crystalline particles in terms of their size distribution, transient stability, and structural organization. In relation, studies on sea urchin spiculogenesis show the inhibition of mineral growth and accumulation of possibly mineralization related vesicles in the presence of protease inhibitors.[38,41] Mechanistic roles of the proteolytic postprocessing of mineralization factors are also evident for other biominerals such as tooth material and magnetosomes.[42,43] Hence, the impacts of the nanoscale bioinorganic interactions between postsynthesis modified macromolecules and distinct mineral phases require attention. On these lines, post-translational modifications such as glycosylation and phosphorylation might have significant impacts on protein-guided pathways of mineral nucleation and crystallization.[15,24,44]

CONCLUSION

This study illuminates the complexity of biochemical and biophysical regulation over the spatiotemporal dynamics of mineral growth and form. The matrix protein SpSM50 emerges as a multifunctional biomineral-associated protein that not only enhances the transient stability of mineral precursors via confinement (based on the liquid−liquid locus[22]) but also assembles organic and inorganic components into mesocrystalline architectures (Figure 4). The contributions of nanoscopic

DOI: 10.1021/acscentsci.8b00853
ACS Cent. Sci. 2019, 5, 357−364

networks and supramolecular assemblies emerge as vital in directing the phase transformations of minerals toward crystalline superstructures.[32,40] During mineralization, the proteolytic processing of structural extracellular proteins with low sequence complexities emerge as crucial for providing optimal inter- and intramolecular interactions that guide the mesoscale self-assembly of inorganic nanocrystals. Isolated from the LCD region, the lectin domain organizes the transient fluidic and possibly particulate[45,46] amorphous mineral precursor into calcitic mesocrystals consisting of polydisperse and irregular, however crystallographically coaligned, mineral particles organized in a space-filling manner. Intertwined with the transformation of highly hydrated amorphous minerals, the mechanism of mesocrystal formation is based on defined bioinorganic interactions affecting the amalgamation and mesoscale assembly of mineral phases and supramolecular assemblies. Given the metastable nature of the mesocrystal structure, the mechanistic roles of transient nanocrystalline domains as intermediates during biogenic and synthetic crystallization also require attention.[47] With proteomic studies revealing diverse sets of biomineral-associated macromolecules,[16] addressing their synergistic functions and relative positions in the regulatory cascade will assist the identification of molecular checkpoints and interactions underlying the integration of supramolecular assembly and mineral growth and structure.[24,48] In addition, with emerging possibilities of performing mineralization reactions at near physiological pH conditions using macromolecules with near native compositional and structural states, the prospects of elucidating critical questions in the field of biomineralization such as the polymorph selectivity of minerals as well as the contributions of bicarbonate species and liquid condensed phases are emerging.[24,49,50] Lastly, the dynamics and ultrastructure of precrystalline entities and stabilizer populations will help further elucidate phase transformation pathways concerning biomineralization.[35,49,51] Further investigations on the synergetic relations between distinct mineral precursors and biomacromolecules under physiological conditions will help resolve nature's blueprint for hierarchical materials, opening avenues for smart additives that control crystallization processes at different length and time scales.

■ ASSOCIATED CONTENT

Supporting Information

The Supporting Information is available free of charge on the ACS Publications website at DOI: 10.1021/acscentsci.8b00853.

Experimental details and supplementary sections (1−8) related to protein expression and purification, mineralization−demineralization methodologies, biochemical assays, and solution and structural analytical investigations (PDF)

Supplementary Video 1: Proteolysis switch for mesocrystal assembly (AVI)

■ AUTHOR INFORMATION

Corresponding Author

*E-mail: Helmut.Coelfen@uni-konstanz.de.

ORCID

Denis Gebauer: 0000-0003-1612-051X

Helmut Cölfen: 0000-0002-1148-0308

Notes

The authors declare no competing financial interest.

Safety Statement: Unexpected or unusual safety hazards were not encountered.

■ ACKNOWLEDGMENTS

A.R. acknowledges a fellowship from Konstanz Research School Chemical Biology. M.D. thanks the Bavarian Polymer Institute and the collaborative research centre SFB840 of the German Research Foundation for financial support. R.K and T.R.-H. acknowledge funding by the European Research Council in the framework of the project SMILEY (FP7-NMP-2012-SMALL-6-310637) and the Engineering and Physical Sciences Research Council (EP/I001514/1). D.G. is a Research Fellow of the Zukunftskolleg, University of Konstanz. We also thank Dr. Joachim Hentschel from the Electron Microscopy Centre; Dr. Andreas Marquardt and Dr. Anna Sladewska-Marquardt from the Proteomics Core Facility, University of Konstanz; and Dr. Alexander Titz, Helmholtz Institute for Pharmaceutical Research Saarland.

■ REFERENCES

(1) Lee, K.; Wagermaier, W.; Masic, A.; Kommareddy, K. P.; Bennet, M.; Manjubala, I.; Lee, S.-W.; Park, S. B.; Cölfen, H.; Fratzl, P. Self-assembly of amorphous calcium carbonate microlens arrays. *Nat. Commun.* **2012**, *3*, 725.

(2) Mao, L.-B.; Gao, H.-L.; Yao, H.-B.; Liu, L.; Cölfen, H.; Liu, G.; Chen, S.-M.; Li, S.-K.; Yan, Y.-X.; Liu, Y.-Y.; et al. Synthetic nacre by predesigned matrix-directed mineralization. *Science* **2016**, *354* (6308), 107−110.

(3) Meldrum, F. C.; Cölfen, H. Controlling mineral morphologies and structures in biological and synthetic systems. *Chem. Rev.* **2008**, *108* (11), 4332−4432.

(4) Sanchez, C.; Arribart, H.; Guille, M. M. G. Biomimetism and bioinspiration as tools for the design of innovative materials and systems. *Nat. Mater.* **2005**, *4* (4), 277.

(5) Oaki, Y.; Imai, H. Nanoengineering in echinoderms: the emergence of morphology from nanobricks. *Small* **2006**, *2* (1), 66−70.

(6) Banfield, J. F.; Welch, S. A.; Zhang, H.; Ebert, T. T.; Penn, R. L. Aggregation-based crystal growth and microstructure development in natural iron oxyhydroxide biomineralization products. *Science* **2000**, *289* (5480), 751−754.

(7) Seto, J.; Ma, Y.; Davis, S. A.; Meldrum, F.; Gourrier, A.; Kim, Y.-Y.; Schilde, U.; Sztucki, M.; Burghammer, M.; Maltsev, S.; et al. Structure-property relationships of a biological mesocrystal in the adult sea urchin spine. *Proc. Natl. Acad. Sci. U. S. A.* **2012**, *109* (10), 3699−3704.

(8) Vidavsky, N.; Addadi, S.; Schertel, A.; Ben-Ezra, D.; Shpigel, M.; Addadi, L.; Weiner, S. Calcium transport into the cells of the sea urchin larva in relation to spicule formation. *Proc. Natl. Acad. Sci. U. S. A.* **2016**, *113*, 12637.

(9) Politi, Y.; Metzler, R. A.; Abrecht, M.; Gilbert, B.; Wilt, F. H.; Sagi, I.; Addadi, L.; Weiner, S.; Gilbert, P. Transformation mechanism of amorphous calcium carbonate into calcite in the sea urchin larval spicule. *Proc. Natl. Acad. Sci. U. S. A.* **2008**, *105* (45), 17362−17366.

(10) Wilt, F. H. Biomineralization of the spicules of sea urchin embryos. *Zool. Sci.* **2002**, *19* (3), 253−261.

(11) Killian, C. E.; Wilt, F. H. Characterization of the proteins comprising the integral matrix of Strongylocentrotus purpuratus embryonic spicules. *J. Biol. Chem.* **1996**, *271* (15), 9150−9159.

(12) Jain, G.; Pendola, M.; Huang, Y.-C.; Gebauer, D.; Evans, J. S. A Model Sea Urchin Spicule Matrix Protein, rSpSM50, Is a Hydrogelator That Modifies and Organizes the Mineralization Process. *Biochemistry* **2017**, *56* (21), 2663−2675.

(13) Jain, G.; Pendola, M.; Rao, A.; Cölfen, H.; Evans, J. S. A model sea urchin spicule matrix protein self-associates to form mineral-modifying protein hydrogels. *Biochemistry* **2016**, *55* (31), 4410−4421.

(14) Rao, A.; Seto, J.; Berg, J. K.; Kreft, S. G.; Scheffner, M.; Cölfen, H. Roles of larval sea urchin spicule SM50 domains in organic matrix self-

DOI: 10.1021/acscentsci.8b00853
ACS Cent. Sci. 2019, 5, 357−364

assembly and calcium carbonate mineralization. *J. Struct. Biol.* **2013**, *183* (2), 205−215.
(15) Jain, G.; Pendola, M.; Koutsoumpeli, E.; Johnson, S. D.; Evans, J. S. Glycosylation fosters interactions between model sea urchin spicule matrix proteins. Implications for embryonic spiculogene-sis and biomineralization. *Biochemistry* **2018**, *57* (21), 3032−3035.
(16) Mann, K.; Wilt, F. H.; Poustka, A. J. Proteomic analysis of sea urchin (Strongylocentrotus purpuratus) spicule matrix. *Proteome Sci.* **2010**, *8* (1), 33.
(17) Addadi, L.; Raz, S.; Weiner, S. Taking advantage of disorder: amorphous calcium carbonate and its roles in biomineralization. *Adv. Mater.* **2003**, *15* (12), 959−970.
(18) De Yoreo, J. J.; Gilbert, P. U.; Sommerdijk, N. A.; Penn, R. L.; Whitelam, S.; Joester, D.; Zhang, H.; Rimer, J. D.; Navrotsky, A.; Banfield, J. F.; et al. Crystallization by particle attachment in synthetic, biogenic, and geologic environments. *Science* **2015**, *349* (6247), aaa6760.
(19) Rao, A.; Drechsler, M.; Schiller, S.; Scheffner, M.; Gebauer, D.; Cölfen, H. Stabilization of Mineral Precursors by Intrinsically Disordered Proteins. *Adv. Funct. Mater.* **2018**, *28* (37), 1802063.
(20) Rao, A.; Cölfen, H. From Solute, Fluidic and Particulate Precursors to Complex Organizations of Matter. *Chem. Rec.* **2018**, *18*, 1203−1221.
(21) Gebauer, D.; Völkel, A.; Cölfen, H. Stable prenucleation calcium carbonate clusters. *Science* **2008**, *322* (5909), 1819−1822.
(22) Sebastiani, F.; Wolf, S. L.; Born, B.; Luong, T. Q.; Cölfen, H.; Gebauer, D.; Havenith, M. Water Dynamics from THz Spectroscopy Reveal the Locus of a Liquid−Liquid Binodal Limit in Aqueous CaCO3 Solutions. *Angew. Chem., Int. Ed.* **2017**, *56* (2), 490−495.
(23) Wilt, F.; Croker, L.; Killian, C. E.; McDonald, K. Role of LSM34/SpSM50 proteins in endoskeletal spicule formation in sea urchin embryos. *Invertebrate Biology* **2008**, *127* (4), 452−459.
(24) Pendola, M.; Jain, G.; Huang, Y.-C.; Gebauer, D.; Evans, J. S. Secrets of the Sea Urchin Spicule Revealed: Protein Cooperativity Is Responsible for ACC Transformation, Intracrystalline Incorporation, and Guided Mineral Particle Assembly in Biocomposite Material Formation. *ACS omega* **2018**, *3* (9), 11823−11830.
(25) Schneider, E. G.; Nguyen, H. T.; Lennarz, W. J. The effect of tunicamycin, an inhibitor of protein glycosylation, on embryonic development in the sea urchin. *J. Biol. Chem.* **1978**, *253* (7), 2348−2355.
(26) Tabbasum, K.; Rao, C. P. Zn 2+ and Cu 2+ induced nanosheets and nanotubes in six different lectins by TEM. *RSC Adv.* **2015**, *5* (22), 16828−16836.
(27) Gower, L. B. Biomimetic model systems for investigating the amorphous precursor pathway and its role in biomineralization. *Chem. Rev.* **2008**, *108* (11), 4551−4627.
(28) Yang, L.; Killian, C. E.; Kunz, M.; Tamura, N.; Gilbert, P. Biomineral nanoparticles are space-filling. *Nanoscale* **2011**, *3* (2), 603−609.
(29) Ma, C. D.; Wang, C.; Acevedo-Vélez, C.; Gellman, S. H.; Abbott, N. L. Modulation of hydrophobic interactions by proximally immobilized ions. *Nature* **2015**, *517* (7534), 347.
(30) Bahn, S. Y.; Jo, B. H.; Choi, Y. S.; Cha, H. J. Control of nacre biomineralization by Pif80 in pearl oyster. *Science advances* **2017**, *3* (8), No. e1700765.
(31) Evans, J. S. Tuning in" to mollusk shell nacre-and prismatic-associated protein terminal sequences. Implications for biomineraliza-tion and the construction of high performance inorganic− organic composites. *Chem. Rev.* **2008**, *108* (11), 4455−4462.
(32) Vidavsky, N.; Addadi, S.; Mahamid, J.; Shimoni, E.; Ben-Ezra, D.; Shpigel, M.; Weiner, S.; Addadi, L. Initial stages of calcium uptake and mineral deposition in sea urchin embryos. *Proc. Natl. Acad. Sci. U. S. A.* **2014**, *111* (1), 39−44.
(33) Cölfen, H.; Völkel, A. Application of the Density Variation Method on Calciumcarbonate Nanoparticles. In *Analytical Ultra-centrifugation VIII*; Springer, 2006; pp 126−128.
(34) Liu, J.; Pancera, S.; Boyko, V.; Shukla, A.; Narayanan, T.; Huber, K. Evaluation of the particle growth of amorphous calcium carbonate in water by means of the porod invariant from SAXS. *Langmuir* **2010**, *26* (22), 17405−17412.
(35) Rao, A.; Huang, Y.-C.; Cölfen, H. Additive Speciation and Phase Behavior Modulating Mineralization. *J. Phys. Chem. C* **2017**, *121* (39), 21641−21649.
(36) Stephens, C. J.; Ladden, S. F.; Meldrum, F. C.; Christenson, H. K. Amorphous calcium carbonate is stabilized in confinement. *Adv. Funct. Mater.* **2010**, *20* (13), 2108−2115.
(37) Wolf, S. E.; Leiterer, J.; Pipich, V.; Barrea, R.; Emmerling, F.; Tremel, W. Strong stabilization of amorphous calcium carbonate emulsion by ovalbumin: gaining insight into the mechanism of 'polymer-induced liquid precursor'processes. *J. Am. Chem. Soc.* **2011**, *133* (32), 12642−12649.
(38) Ingersoll, E. P.; Wilt, F. H. Matrix metalloproteinase inhibitors disrupt spicule formation by primary mesenchyme cells in the sea urchin embryo. *Dev. Biol.* **1998**, *196* (1), 95−106.
(39) Mao, Y.; Satchell, P. G.; Luan, X.; Diekwisch, T. G. SM50 repeat-polypeptides self-assemble into discrete matrix subunits and promote appositional calcium carbonate crystal growth during sea urchin tooth biomineralization. *Ann. Anat.* **2016**, *203*, 38−46.
(40) Gong, Y. U.; Killian, C. E.; Olson, I. C.; Appathurai, N. P.; Amasino, A. L.; Martin, M. C.; Holt, L. J.; Wilt, F. H.; Gilbert, P. Phase transitions in biogenic amorphous calcium carbonate. *Proc. Natl. Acad. Sci. U. S. A.* **2012**, *109* (16), 6088−6093.
(41) Ingersoll, E. P.; Mcdonald, K. L.; Wilt, F. H. Ultrastructural localization of spicule matrix proteins in normal and metalloproteinase inhibitor-treated sea urchin primary mesenchyme cells. *J. Exp. Zool.* **2003**, *300* (2), 101−112.
(42) Hershey, D. M.; Ren, X.; Melnyk, R. A.; Browne, P. J.; Ozyamak, E.; Jones, S. R.; Chang, M. C.; Hurley, J. H.; Komeili, A. MamO is a repurposed serine protease that promotes magnetite biomineralization through direct transition metal binding in magnetotactic bacteria. *PLoS Biol.* **2016**, *14* (3), No. e1002402.
(43) Fincham, A.; Hu, Y.; Lau, E.; Slavkin, H.; Snead, M. Amelogenin post-secretory processing during biomineralization in the postnatal mouse molar tooth. *Arch. Oral Biol.* **1991**, *36* (4), 305−317.
(44) Wojtas, M.; Wołcyrz, M.; Ozyhar, A.; Dobryszycki, P. Phosphorylation of intrinsically disordered starmaker protein increases its ability to control the formation of calcium carbonate crystals. *Cryst. Growth Des.* **2012**, *12* (1), 158−168.
(45) Radha, A.; Forbes, T. Z.; Killian, C. E.; Gilbert, P.; Navrotsky, A. Transformation and crystallization energetics of synthetic and biogenic amorphous calcium carbonate. *Proc. Natl. Acad. Sci. U. S. A.* **2010**, *107* (38), 16438−43.
(46) Politi, Y.; Arad, T.; Klein, E.; Weiner, S.; Addadi, L. Sea urchin spine calcite forms via a transient amorphous calcium carbonate phase. *Science* **2004**, *306* (5699), 1161−1164.
(47) Mastropietro, F.; Godard, P.; Burghammer, M.; Chevallard, C.; Daillant, J.; Duboisset, J.; Allain, M.; Guenoun, P.; Nouet, J.; Chamard, V. Revealing crystalline domains in a mollusc shell single-crystalline prism. *Nat. Mater.* **2017**, *16*, 946.
(48) Jain, G.; Pendola, M.; Huang, Y.-C.; Gebauer, D.; Koutsoumpeli, E.; Johnson, S.; Evans, J. S. Selective Synergism Created by Interactive Nacre Framework-Associated Proteins Possessing EGF and vWA Motifs: Implications for Mollusk Shell Formation. *Biochemistry* **2018**, *57* (18), 2657−2666.
(49) Ibsen, C. J. S.; Gebauer, D.; Birkedal, H. Osteopontin Stabilizes Metastable States Prior to Nucleation during Apatite Formation. *Chem. Mater.* **2016**, *28* (23), 8550−8555.
(50) Bewernitz, M. A.; Gebauer, D.; Long, J.; Cölfen, H.; Gower, L. B. A metastable liquid precursor phase of calcium carbonate and its interactions with polyaspartate. *Faraday Discuss.* **2012**, *159* (1), 291−312.
(51) Xu, Y.; Tijssen, K. C.; Bomans, P. H.; Akiva, A.; Friedrich, H.; Kentgens, A. P.; Sommerdijk, N. A. Microscopic structure of the polymer-induced liquid precursor for calcium carbonate. *Nat. Commun.* **2018**, *9* (1), 2582.

DOI: 10.1021/acscentsci.8b00853
ACS Cent. Sci. 2019, 5, 357−364